Balloon Pin-Array Gripper: Two-Step Shape Adaptation Mechanism for Stable Grasping Against Object Misalignment

Yuto Kemmotsu[®], *Graduate Student Member*, *IEEE*, Kenjiro Tadakuma[®], Kazuki Abe[®], *Member*, *IEEE*, Masahiro Watanabe[®], *Member*, *IEEE*, and Satoshi Tadokoro[®], *Fellow*, *IEEE*

Abstract—This letter introduces a balloon pin-array gripper combining shape adaptability to various objects, stable holding by multipoint contact, and isotropic grasping performance. This is particularly useful when the shape or position of the objects cannot be accurately determined because of sensor limitations. This gripper has multiple pins whose tips are covered by flexible balloons. The gripper can adapt to the shapes of objects in two steps: axial sliding of the pins and radial inflation of the balloons. This study focuses on the effect of the layout of pins on grasping and proposes a simulation model to quantify the characteristics of each layout. Simulations showed that the concentric layout enables stable grasping by ensuring many pins contact the object, regardless of misalignment. Experiments using a prototype gripper demonstrated a trend consistent with the simulation results, proving the validity of the simulation model.

Index Terms—Compliant joints and mechanisms, grasping, soft robot materials and design.

I. INTRODUCTION

ROBOTIC grasping remains a challenge in several situations. The grasping difficulty varies significantly depending on the geometry and poses of the objects; hence, robots should acquire such information before grasping, formulate grasping strategies, and be precisely controlled. Therefore, grasping tasks become more difficult when robots handle a wide variety of unfamiliar objects, such as in high-mix, low-volume production.

Recently, the demand for universal grasping with simpler mechanisms and controls has motivated research into fingered

Received 29 April 2024; accepted 15 August 2024. Date of publication 6 September 2024; date of current version 18 September 2024. This article was recommended for publication by Associate Editor B. Sundaralingam and Editor J. Borràs Sol upon evaluation of the reviewers' comments. This work was supported by JSPS KAKENHI under Grant JP23KJ0217. (Corresponding author: Kenjiro Tadakuma.)

Yuto Kemmotsu and Satoshi Tadokoro are with the Graduate School of Information Sciences, Tohoku University, Sendai 980-8577, Japan (e-mail: kemmotsu.yuto@rm.is.tohoku.ac.jp; tadokoro@rm.is.tohoku.ac.jp).

Kenjiro Tadakuma is with the Graduate School of Information Sciences, Tohoku University, Sendai 980-8577, Japan, and also with the Graduate School of Engineering Science, Osaka University, Osaka 565-0871, Japan (e-mail: kenjiro.tadakuma.es@osaka-u.ac.jp).

Kazuki Abe and Masahiro Watanabe are with the Graduate School of Engineering Science, Osaka University, Osaka 565-0871, Japan (e-mail: kazuki.abe.es@osaka-u.ac.jp; watanabe.masahiro.es@osaka-u.ac.jp).

This letter has supplementary downloadable material available at https://doi.org/10.1109/LRA.2024.3455850, provided by the authors.

Digital Object Identifier 10.1109/LRA.2024.3455850

grippers made of soft materials. Actuation methods include the pneumatic drive [1], [2], [3], [4], [5], fin-ray effect [6], electrostatic [7], electromagnetic [8], magnetorheological fluid [9], and gecko-inspired adhesion [10]. Compliant interactions enable grippers to handle objects of different geometries and fragility with the same planning and control. However, anisotropy in grasping performance is inevitable when grasping with fingers. To make the fingers contact the objects at more points and grasp them stably, the gripper has to approach objects by considering the relative positions of the fingers and objects.

Nonfingered grippers with less anisotropy have also been proposed. Typical designs include bladder-shaped grippers with variable stiffness mechanisms by granular jamming [11], [12], [13], magnetorheological fluid [14], or low-melting-point alloy [15]. Their axisymmetric shapes enable these grippers to have a constant grasping performance regardless of their orientation; moreover, they can tolerate some offset in the positions of the objects. However, contact and shape adaptation are achieved by passively deforming the bladders against objects, limiting the holding force as the bladders cannot actively generate a contact force against the sides of the objects.

Other shape-adaptive nonfingered grippers envelop objects from the periphery. These include an origami-structured hollow hemispherical gripper [16], gripper with a cylindrical array of parallel chambers in a soft accordion structure [17], and gripper that inwardly expands a chamber located on the inner wall of a cylinder [18]. These grippers can envelop a part or the entire object while deforming to adapt to the shape of the object; therefore, they can be expected to provide stable grasping with a large contact area regardless of their orientation. However, objects that can be enveloped are limited to those smaller than the gripper's maximum diameter, and larger objects need to be handled with additional functions such as suction. For example, grasping the tips of bottles has been reported in these studies; however, grasping them when they collapse is difficult.

Grippers with passively sliding pin arrays are another configuration that can reduce anisotropy while providing shape adaptability depending on the density of the pin array, and several methods have been proposed for this. Although the early method of grasping by bringing two sets of pin arrays close together [19] or tilting the pins in the center of the gripper [20] may fail to grasp objects in a specific position or orientation, recent studies have proposed other pin array designs to resolve the anisotropy, for example, a gripper whose pins are arranged on concentric rings that can be rotated [21] and a gripper that rotates pins with elliptical cross sections [22]. However, owing

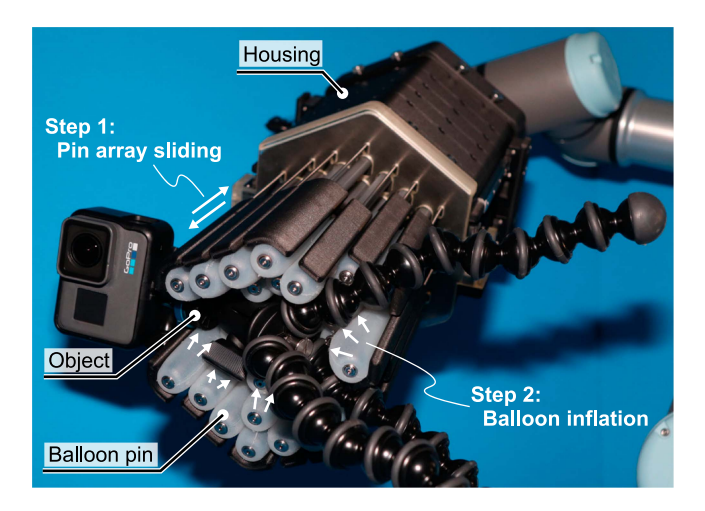


Fig. 1. Prototype of balloon pin-array gripper grasping a camera with tripod. By covering the pins with flexible balloons, this gripper can adapt to the shape of objects in two steps: Sliding the pin array and inflating the balloons.

to the directionality of the pin movements to generate a grasping force, the number of pins that can contact the objects is limited. Furthermore, the pins cannot adapt to the lateral geometry of an object because the contact points are rigid. Therefore, the limited number of contact points leads to localized load concentration and unstable grasping issues.

In this study, we propose a balloon pin-array gripper (Fig. 1) that combines shape adaptability to various objects, stable holding by multipoint contact, and isotropic grasping performance. This gripper has a flexible balloon mounted on the tip of each pin that makes up a pin array and can adapt to the shapes of objects in two steps: axial sliding of the pins, and radial inflation of the balloons. Approaching the surfaces of objects in multistep motion enables them to contact many points or surfaces of objects of various shapes. Moreover, it enables generation of a constant holding force regardless of the orientation of the gripper because balloon inflation is not directional.

The balloon pin-array gripper has two characteristics that should be clarified.

- 1) Effect of the second step of the shape adaptation on the sides of the objects owing to balloon inflation
- 2) Relationship between the layout of the pins and isotropy of grasping performance

The first point was partially clarified in our previous study [23], with experimental results showing that the holding force increased as the balloon adapted to the geometry of the sides of the objects. This study focuses on the second point, benchmarking the isotropy of the grasping performance by simulations using a simple model and clarifying the differences in characteristics depending on the pin layout. Furthermore, the simulation method was validated through experiments using a prototype gripper.

The remainder of the study is organized as follows. Section II describes the basic configuration and grasping method of the balloon pin-array gripper. Section III proposes a simulation method to quantify the isotropy of the grasping performance; the characteristics of each pin layout are discussed based on the simulation results. Section IV presents the results of experiments with a prototype to validate the simulations. The interpretation of the simulation and experimental results and further research topics are discussed in Section V, followed by the conclusion in Section VI.

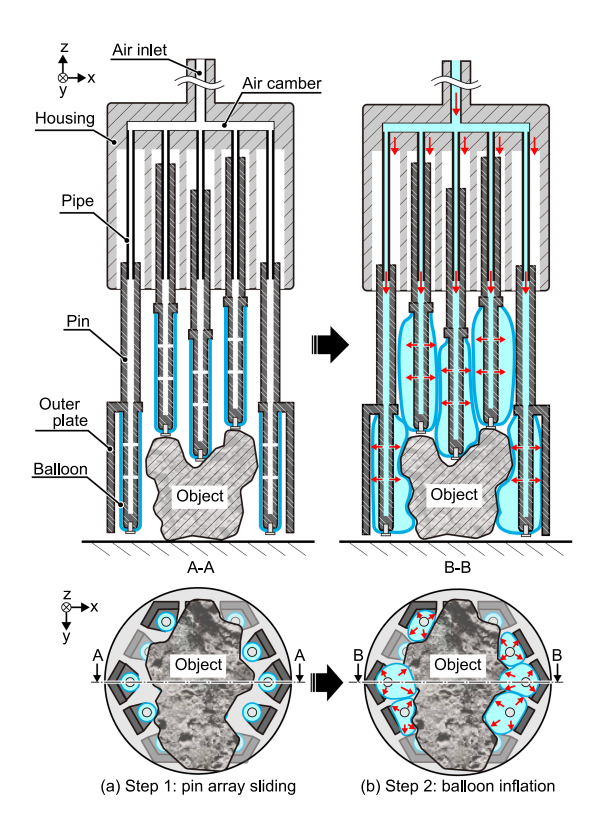


Fig. 2. Basic configuration and grasping procedure of the balloon pin-array gripper. The grasping procedure involves two sequential steps: (a) Step 1, the pin array is pressed against an object. (b) Step 2, the balloons are inflated with air to fill the space around the object and grasp it.

II. CONCEPT OF THE BALLOON PIN-ARRAY GRIPPER

The proposed gripper mainly consists of a pin array and housing, with the tip of each pin covered by a tubular balloon. The ends of the tubular balloons are attached to pins that enable the balloons to inflate radially while preventing axial extension. The pins are sufficiently hollow to supply air to the balloons. An air supply pipe was inserted into each pin to provide a flow path even when the pins slide. These air supply pipes were connected to a single air inlet by an air chamber in the housing, which simultaneously supplied air to all balloons. The outer plates were attached to the outermost pins of the pin array to limit inward balloon inflation and apply a grasping force to the object. The grasping procedure using the proposed gripper involves two sequential steps: sliding the pin array and inflating the balloons. In Step 1 (Fig. 2(a)), the pin array was pressed against an object without supplying air to the balloons. Passive sliding of the pin array in contact with the object resulted in shape adaptation in the z-direction. However, at this point, gaps remained between the pins and the side of the object. In Step 2 (Fig. 2(b)), air was supplied to the balloons to inflate them in the radial direction of each pin. This caused shape adaptation in the x- and y-directions, and the inflated balloons filled the gaps between the pins and object in Step 1.

This grasping method was expected to combine shape adaptability to various objects, stable holding by multipoint contact, and isotropic grasping performance. The two-step approach to object surfaces using a pin array and balloons is expected to enable contact with many points or surfaces, regardless of the shape of the object. In addition, balloon inflation, which performs Step 2 of shape adaptation, is not directional and fills the surrounding space, which reduces the difference in the

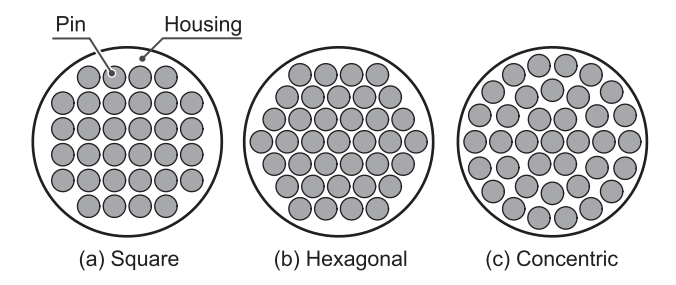


Fig. 3. Examples of balloon pin layouts.

number of contact points and holding force depending on the orientation of the gripper. This method should be adequate for objects of a certain height; however, it is necessary to consider that the balloons cannot make significant contact with the sides of objects of low height, such as thin-plate objects. The isotropy of the grasping performance is expected to be affected by the pin layout, as discussed in Section III.

III. EVALUATION OF BALLOON PIN LAYOUT

A. Requirements for Layout of Balloon Pins

The three expected characteristics of the balloon pin-array gripper listed in the previous section—high shape adaptability, stable holding by multipoint contact, and isotropic grasping performance—are expected to be influenced by the layout of the balloon pins. To increase the resolution of the shape adaptation and enable multipoint contact with objects of different shapes, the pins should be placed more densely. In addition, the pin array itself should be isotropic to reduce directional dependence.

Three examples of simple pin layouts (square, hexagonal, and concentric) are shown in Fig. 3. They have the same housing diameter, pin diameter, and minimum pin-to-pin spacing. However, there are differences in the pin density (the number of pins placed in a housing of the same diameter) and isotropy.

The square layout in Fig. 3(a) has the lowest pin density among the three layouts and is anisotropic because the contours of the entire pin array are square. While grasping a rod-shaped object, the number of pins that can make contact with the object varies depending on whether the object is positioned horizontally or diagonally.

The hexagonal layout in Fig. 3(b) and the concentric layout in Fig. 3(c) have the same number of pins arranged under the housing and pin diameters. However, the spacing between the pins is different. In the hexagonal layout, the spacing between adjacent pins is constant, whereas in the concentric layout, the spacing is relatively wide. However, the contour of the entire pin array is hexagonal in the hexagonal layout, whereas it is circular in the concentric layout; therefore, isotropy is superior in the concentric layout.

The difference in the characteristics owing to the layout may be smaller when the pins are thinner and the number of pins is larger. However, balloon pins require relatively large diameters because they require internal flow paths. Therefore, the selection of an appropriate layout method is more critical than the selection of conventional pin-array grippers with thin pins.

B. Simulation Model to Evaluate Pin Layouts

To achieve stable holding by multipoint contact, one of the performance indicators of the proposed gripper is the number of balloon pins that can contact an object. Therefore, we propose

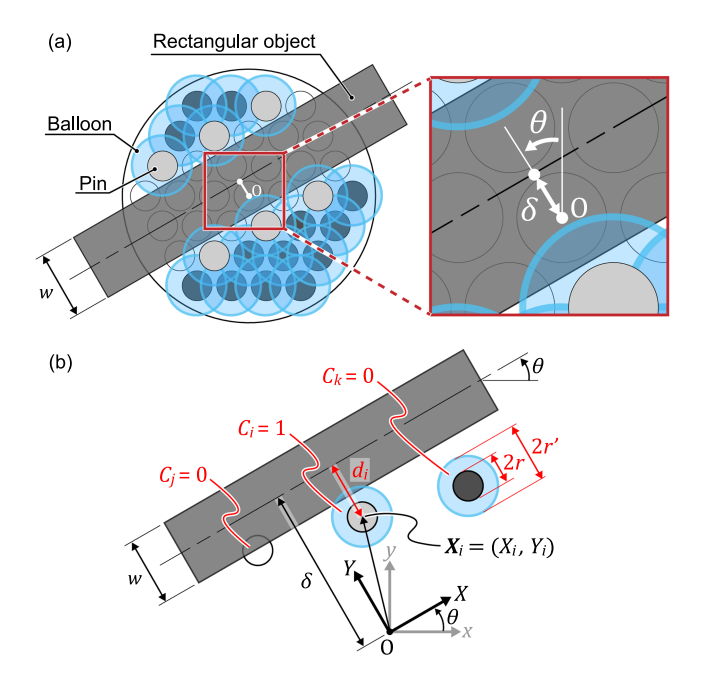


Fig. 4. Geometric model to calculate the number of contactable balloon pins. (a) Contact judgment made on a plate-shaped object. In this diagram, the six light gray pins are considered contactable. (b) Criteria of the contact judgment based on the distance between each pin and the object.

a method for calculating the number of contactable pins using a geometric model representing a two-step shape adaptation to compare the differences in grasping performance depending on the pin layout.

Fig. 4(a) shows the model used to calculate the number of contactable pins. The blue circular area surrounding each pin represents the balloon after inflation and the gray rectangle represents the object. In this model, each balloon is assumed to inflate concentrically to a certain pin radius, and the balloon pin is considered to be in contact with the object when the blue area representing the balloon after inflation overlaps with the object. Pins that partially or entirely overlap with the object are drawn transparently and not counted as contactable pins because they slide when the pin array is pressed against the object (Step 1).

A plate-shaped object (rectangular from the bottom of the gripper) with a length greater than the gripper diameter was assumed as the target object and angle θ ; the offset δ from the gripper center, and the width w were set as parameters. With this setup, the simulation results were expected to reflect the effects of the pin density and isotropy of the layouts. The number of contactable pins should not vary significantly with θ and δ to achieve multipoint contact regardless of the position and orientation of the object.

Fig. 4(b) illustrates the criteria for determining contact between the balloon pins. The radii of the pins before and after balloon inflation are r and r', respectively. The distance between the center line l of the object and the center of the i-th pin $(i \in \mathbb{N}, \ 1 \le i \le N)$ of the total N pins in the pin array is denoted as d_i , which varies depending on the pin layout and the angle and offset of the object.

To obtain d_i , consider an X-Y coordinate system rotated by an angle θ concerning the x-y coordinates whose origin is the center O of the gripper. Subsequently, the equation of the object

TABLE I PARAMETERS USED FOR THE SIMULATIONS

Gripper dimensions	
Housing diameter	110 mm
Pre-inflation diameter of pins 2r	13 mm
Post-inflation diameter of balloons $2r'$	26 mm
Minimum pin spacing	15 mm
Parameters of the rectangular object	
Width w	15, 20, 25, 30 mm
Angle θ	0° to 90° in 0.1° increments
Offset δ	0% to 20%
(percentage of the housing diameter)	in 0.02 % increments

centerline l can be expressed as

$$Y = \delta \tag{1}$$

in the X-Y coordinate system. The coordinates of the i-th pin in the x-y coordinate system $x_i = (x_i, y_i)$ are transformed into the coordinates $X_i = (X_i, Y_i)$ in the X-Y coordinate system, which are expressed using a rotation matrix $R(\theta)$ as

$$\boldsymbol{X}_{i} = \boldsymbol{R}\left(-\theta\right)\boldsymbol{x}_{i} \tag{2}$$

Thus, the distance d_i between the object's centerline l and the center of the i-th pin is given by the difference in the Y coordinates as follows:

$$d_i = |Y_i - \delta|. (3)$$

Let C_i be a variable that indicates the result of determining whether the i-th balloon pin is contactable. Because the balloon pin can contact the object if the pin does not slide (does not overlap with the object) in Step 1, and the object is located within the balloon inflation area in Step 2, C_i is expressed as

$$C_i = \begin{cases} 1, & \text{if } r + \frac{w}{2} < d_i \le r' + \frac{w}{2} \\ 0, & \text{otherwise.} \end{cases}$$
 (4)

The number of contactable balloon pins n is calculated by taking the sum of C_i in the range $1 \le i \le N$ as follows:

$$n = \sum_{i=1}^{N} C_i. (5)$$

Here, the total number of pins N varies with the layout.

The values of the parameters used in the simulations are listed in Table I. The minimum pin spacing was set to 15 mm for a pin diameter of 13 mm, and the maximum number of pins was placed in a circular housing with a diameter of 110 mm, according to each layout. The dimensions were determined based on the prototype design built in our previous study [23]. The post-inflation diameter of balloon 2r', was set to twice the pre-inflation diameter 2r. This value can be larger depending on the balloon material and internal pressure; however, it was set at this value because, if it is extremely large, a balloon that is expected to interfere with other balloon pins will be judged to be contactable. The object width w was set to four different values, and the calculations were performed by moving the object in the range $0^{\circ} \le \theta \le 90^{\circ}$ and $0\% \le \delta \le 20\%$. If δ was extremely large that the balloon pin could contact only one side of the object, n was not calculated because the gripper could not grasp the object.

C. Simulation Results

Fig. 5 shows heat maps of the simulation results for the three layouts shown in Fig. 3. In these heat maps, the horizontal axis was θ , and the vertical axis was δ . The color from blue to yellow represents the number of contactable pins n when the object was placed at the position determined by θ and δ . The white area indicates where the offset of the object was extremely large to be grasped. Four different results are shown for each layout depending on the width w of the object.

The heat map for the square layout (Fig. 5(a)–(d)) showed a relatively large area of cold color, that is, small n, probably because of the smaller number of pins compared to the other two layouts. In addition, n changed drastically around $\theta = 0^{\circ}$ and 90° , particularly noticeable at w = 25 mm (Fig. 5(c)). Fig. 6 illustrates the positional relationship between the gripper and object when n is small. In Step 1, the object in this position slides through many pins and was far from any other pin, probably because the objects and rows of pins could have been parallel in square layouts where the pins are arranged linearly in the 0° and 90° directions. The ungraspable area was also larger around $\theta = 0^{\circ}$ and 90° (Fig. 5(c) and (d)) because the pins in the outermost rows had different distances from the gripper center depending on the angle. Such extreme changes in n at certain angles can be considered a reflection of the anisotropic nature of the pin layout.

The hexagonal layout had a wider warm-colored area (Fig. 5(e)–(h)) than the other two layouts, confirming the effect of the denser pin arrangement. However, at w=20 and 30 mm (Fig. 5(d), (h)), n changed drastically around $\theta=0^\circ$ and 60° , suggesting that the grasping performance was anisotropic. Fig. 6(b) illustrates the gripper and the object in this case. As in the square layout case, the object was parallel to the straight line where the pins were arranged. The larger ungraspable area at $\theta=0^\circ$ and 60° was also similar to that of the square layout.

The heat map of the concentric layout (Fig. 5(i)–(l)) showed a relatively large area of cold color because this layout has a lower pin density than the hexagonal layout. However, the variation in n with angle was slight, and the ungraspable area was also smaller, reflecting the highly isotropic property.

From the above results, differences in the characteristics depending on the layout were visualized, such as the fact that the hexagonal layout, which is the densest layout, is not necessarily optimal owing to its anisotropic nature. However, whether the model reflects the actual grasping characteristics is not clear because it does not consider the mechanical interaction between the gripper and the object. The following section describes experiments using a prototype to verify the validity of the simulation model.

IV. EXPERIMENTS

A. Design of Experimental Prototype

The prototype balloon pin-array gripper fabricated for the experiments is shown in Figs. 1 and 7. A hexagonal layout was used for the pin layout of the prototype, which showed an area of extreme variation in n in Fig. 5(f) and (h). This was performed to confirm whether the grasping performance of the actual machine changed significantly depending on the position of the object, as in the simulations. The number of balloon pins in the prototype was 37, as shown in Fig. 3(b).

Table II lists the specifications of the prototype. Balloon pins with diameters of 13 mm were arranged at a spacing of 15 mm,

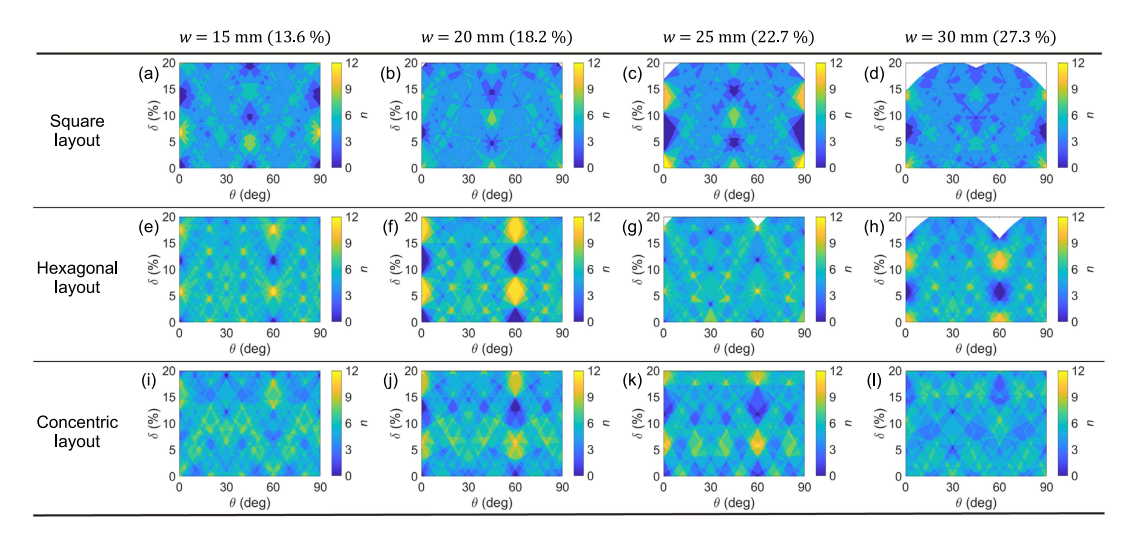


Fig. 5. Heat maps of the number of contactable pins n when the object was placed at the position determined by θ and δ . The white area is where the offset of the rectangular object was too large to grasp it. The values listed next to the object's width w are the percentages of the housing diameter.

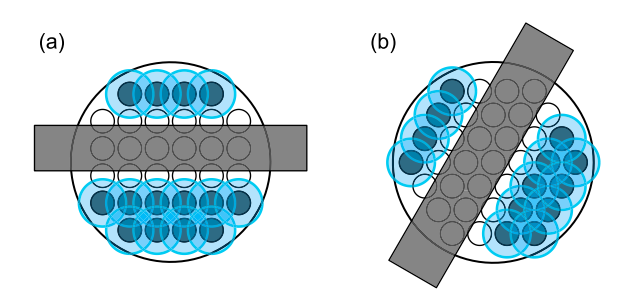


Fig. 6. Examples of the situations where the number of contactable pins is small. (a) Square layout at w=25 mm, $\theta=0^\circ$ and $\delta=7\%$. (b) Hexagonal layout at w=30 mm, $\theta=60^\circ$ and $\delta=7\%$.

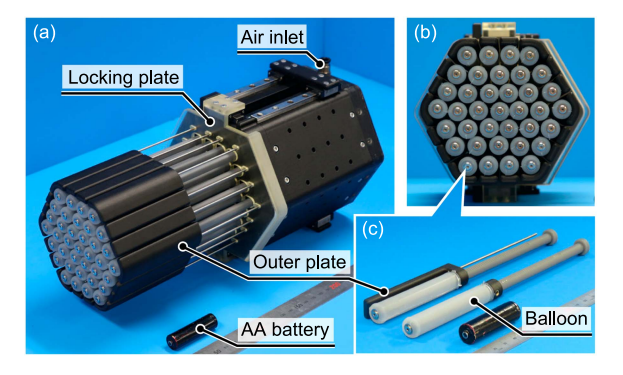


Fig. 7. (a) Oblique view of the prototype balloon pin-array gripper. (b) Pin array designed in a hexagonal layout. (c) Balloon pins (with and without the outer plate) used in the prototype.

similar to the parameters used in the simulations. Most parts were 3D printed using Onyx (Markforged Inc., chopped carbon-fiber-reinforced nylon).

Fig. 8 illustrates the structure of the balloon pin. The pin was divided into a balloon mount and sliding part for ease of assembly, and both parts were connected by a set screw. The balloon mount, made of Onyx, was covered by a balloon that was fixed to the balloon mount with a polyurethane thread at the top and a screw at the bottom. The balloons were fabricated by pouring Dragon Skin 10 medium (Smooth-On, Inc.), an easy-to-mold silicone rubber, into a tubular mold made using a 3D

TABLE II SPECIFICATIONS OF THE PROTOTYPE GRIPPER

Whole body	Dimensions	147 × 160 × 320 mm
	Mass	2.4 kg
Housing	Layout of pin array	Hexagonal layout
	Number of pins	37
	Spacing between pins	15 mm
	Mass	1.5 kg
Pin	Outer diameter	13 mm
	Sliding range	70 mm
	Mass (w/o outer plate)	20 g
	Mass (w/ outer plate)	31 g (corners), 27 g (others)
Balloon	Material	Silicone rubber
		(Dragon Skin 10 medium)
	Thickness	1.5 mm
	Length along axis	80 mm

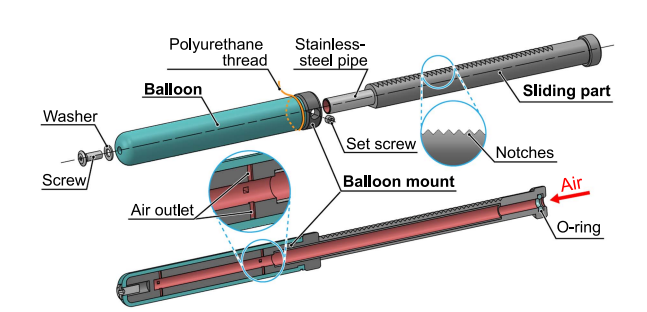


Fig. 8. Structure of the balloon pin.

printer. The inside of the pin was hollow, and air was supplied to the balloon through the air outlets on the side of the balloon mount. The sliding part was 3D printed with Gray Pro Resin (Formlabs Inc.) to provide a notch for locking the pin slide. A stainless-steel pipe was glued to the inside of the sliding part to compensate for stiffness.

Fig. 9 illustrates the internal structure of the prototype gripper. Inside the housing that held the pins, a stainless-steel pipe for air supply was inserted into each pin using an O-ring, allowing air to be supplied even when the pins were sliding. These pipes were connected to a single air chamber and an air inlet at the top of the housing such that the same pressure was applied to all the balloon pins simultaneously. A locking plate attached to

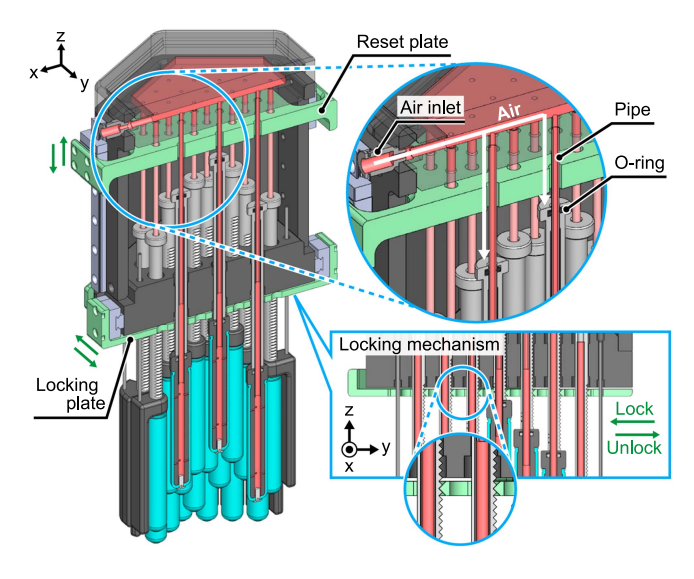


Fig. 9. Internal structure of the prototype gripper.

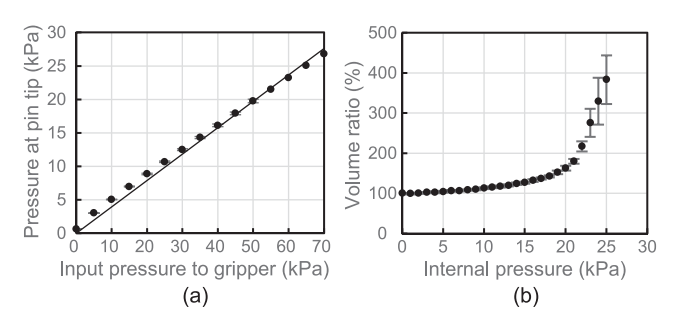


Fig. 10. (a) Pressure transmitted to the pin tip relative to the input pressure to the gripper. (b) Expansion rate of balloons relative to their internal pressure.

the bottom of the housing could slide horizontally and engage with a notch on the side of the pin to lock the pins in position after shape adaptation. The pins could be returned to their initial positions after being grasped by sliding the reset plate vertically and pressing the ends of the pins.

Fig. 10 illustrates the pneumatic characteristics of the prototype gripper. First, the pressure transmitted to the balloon relative to the input pressure to the gripper was measured. This was performed by disconnecting the balloon mount from one pin of the gripper and connecting the pressure gauges (SMC, ZSE30AF-C6H-N-M) to the tip of the pin and air inlet. The same measurements were repeated five times by changing the pin to which the pressure gauge was connected. The measurement results are shown in Fig. 10(a). The pressure transmitted to the pin tip increased linearly with the input pressure to the gripper, with an input-output ratio of 39%.

Subsequently, the expansion rates of the balloons were measured against the pressure transmitted to the balloon mount. To measure the expansion rate, a balloon mount was connected directly to an air regulator and a pressure gauge. The inflated balloon was submerged in water, and the buoyancy force was measured using an electronic balance (A&D, EK-4100i) to calculate the volume. The same measurements were performed on five different balloon mounts covered with balloons used in the prototype gripper. The results are shown in Fig. 10(b). The balloons were inflated to approximately 400% of their pre-inflated volumes when a pressure of 25 kPa was applied. However, there was a greater variation in the expansion rate



Fig. 11. Grasping tests using the prototype. (a) Aluminum frame (343 g). (b) Screwdriver (95 g). (c) Flashlight (363 g). (d) Splay can (83 g). (e) Curing tape (102 g). (f) Flashlight with a handle (768 g).

between individual balloons as the pressure increased, possibly owing to differences in balloon thickness during the molding process.

To summarize the results in Fig. 10, applying 65 kPa to the gripper transferred approximately 25 kPa (39% of the input) to the balloon, inflating it by approximately 400%.

Several grasping tests were conducted using the prototype gripper (Fig. 11). The gripper was pressurized to 65 kPa to grasp any object shown in the figure. The gripper could grasp objects of various shapes, including rod-shaped objects that were longer than the diameter of the gripper (Fig. 11(a)–(c)) and cylindrical objects (Fig. 11(d)). The curing tape shown in Fig. 11(e) was grasped by multiple balloon pins contacting each of the inner and outer walls of the hole, confirming the grasping behavior owing to the omnidirectional nature of balloon inflation. The flashlight shown in Fig. 11(f) was grasped by balloons biting into the handle. This action of approaching the side of an object and adapting to its shape is not possible using conventional pin-array grippers.

However, convex objects such as balls were caught in the pin array and could not be released, even when the balloons were deflated. Moreover, low-height objects such as pens or scissors could not be grasped owing to insufficient contact force, suggesting the disadvantage of using a pin array. Further experiments are required to distinguish objects that can be grasped by improving the gripper design from those that are fundamentally difficult to grasp using the proposed method.

B. Methods

We measured the holding force of the prototype based on the position and orientation of the plate-shaped object, as in the simulations, using the experimental setup shown in Fig. 12. The gripper was mounted on a rotary stage and X-axis stage to adjust the angle and offset. The plate-shaped object was rectangular with a width of w, as viewed from the top, and had a height of 70 mm, which is the same as the sliding range of the pins. The object was mounted on a frame with linear guides and could move only vertically.

The experimental procedure was as follows:

i) The angle θ and offset δ of the gripper relative to the object were adjusted using rotary and X-axis stages.

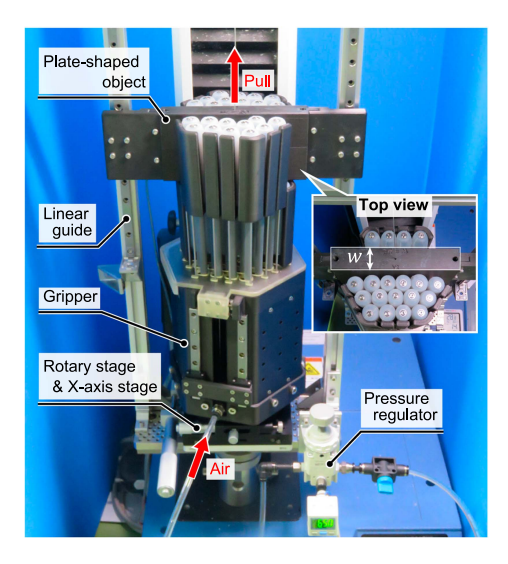


Fig. 12. Experimental setup to measure the holding force depending on the position and orientation of the object.

- The object was moved along the linear guides and pressed against the gripper to slide the pins.
- iii) A pressure of 65 kPa was applied to the gripper to grasp the object.
- iv) The object was pulled using a tensile tester (INSTRON, Model 3343) at a speed of 100 mm/min, and the peak force minus the gravity of the specimen was measured as the maximum holding force.
- v) Steps (ii) through (iv) were repeated for a total of 5 measurements.
- vi) The gripper angle and offset were changed, and steps (ii)-(v) were repeated.

The input pressure in step (iii) was set at 65 kPa to inflate the balloons to approximately twice their diameter, as in the simulations. The balloons were inflated to approximately 400% volume when 65 kPa was applied to the prototype (Fig. 10). Assuming that the balloons inflated only in the radial direction because of the restraints at both ends, the diameter was approximately twice as large when inflated to 400%.

The object width w was changed to 20 mm and 25 mm to compare the behavior of the prototype with that of the simulations by conducting experiments under conditions where extreme color changes appeared in the heat map (Fig. 5(f)) and where extreme color changes did not appear (Fig. 5(g)). The angle θ between the gripper and object was varied from 0° to 90° in 30° increments, and the offset δ was varied from 0 to 15% in 3% increments of the 110 mm that was the housing diameter in the simulations.

C. Results

Fig. 13 shows a comparison of the number of contactable pins n calculated in the simulations with the measured holding force F. The heat maps in Fig. 5 corresponding to each experimental condition are shown in Fig. 13(a-1) and (a-2). The graphs are color-coded in two ways because n had the same value at $\theta=0^\circ$ and 60° and at $\theta=30^\circ$ and 90° respectively, owing to the symmetry of the hexagonal layout.

When w=20 mm (Fig. 13(b-1)), the simulation results showed a large increment in n at $\theta=0^\circ$ and 60° , while the increase was relatively small at $\theta=30^\circ$ and 90° . The experimental results showed a similar trend, with F at $\theta=0^\circ$ and 60°

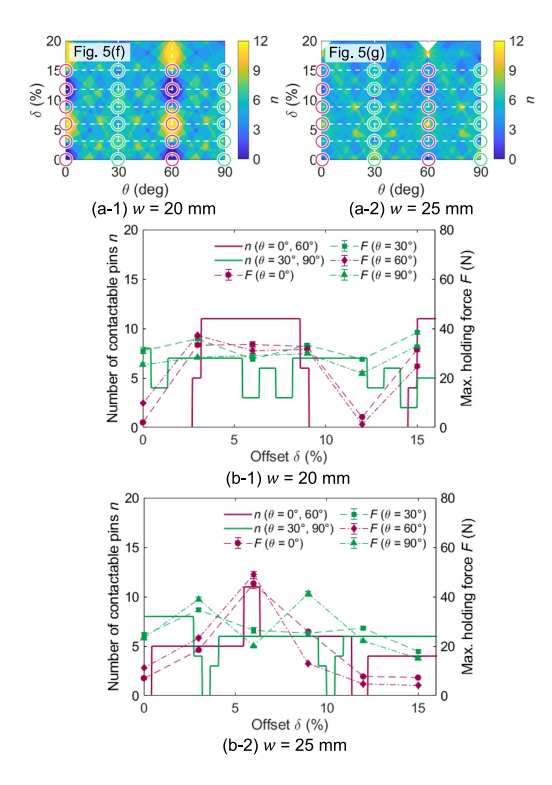


Fig. 13. (a-1), (a-2) Heat maps in Fig. 5 corresponding to each experimental condition. (b-1), (b-2) comparison of the number of contactable pins n calculated in the simulations (solid lines) with the measured holding force F (line graphs with dashed lines).

decreasing significantly to approximately 5 N for $\delta=0\%$ and 12%, while F at $\theta=30^\circ$ and 90° remained at approximately 30 N regardless of δ . However, in the simulations, there was a difference in n between $\theta=0^\circ$, 60° and $\theta=30^\circ$, 90° around $3\% \leq \delta \leq 9\%$, while in the experiments, there was no significant difference in F in that range. Furthermore, F increased at $\delta=15\%$ for $\theta=30^\circ$ and 90° , which was also a different trend from the simulation. These differences may be because the model shown in Fig. 4 does not consider mechanics.

When w=25 mm (Fig. 13(b-2)), the simulation results showed that for $\theta=0^\circ$ and 60° , n had significant changes locally around $\delta=0\%$, 6%, and 12%, while for $\theta=30^\circ$ and 90° , n was almost constant except around $\delta=3\%$ and 10%. The experimental results showed that for $\theta=0^\circ$ and 60° , F was small for $\delta=0\%$ and 12% and large for $\delta=6\%$, while for $\theta=30^\circ$ and 90° , F had few significant changes except for $\delta=9\%$, confirming a similar trend to n. When $\delta=9\%$, where F differed between $\theta=30^\circ$ and 90° , the number of pins sliding in step (ii) of the experimental procedure was different because some of the pins in the prototype were slightly tilted. This suggests that the fabrication accuracy of the pin array can significantly affect the gripper characteristics.

V. DISCUSSION

The validity of the simulation method described in Section III was demonstrated by the fact that the simulation predicted the position and orientation of an object that significantly increased or decreased the holding force in the experiment described in Section IV. Thus, the proposed simulation method can be used to identify the advantages and disadvantages of each pin layout. Although the axial holding force of the pins was used as an

evaluation index in this experiment, the holding force and torque for the other five axes should be evaluated in the future.

Based on the simulation results presented in Section III, we believe that the concentric layout is superior among the three candidates shown in Fig. 3. This is because the concentric layout has the second highest pin density after the hexagonal layout, and it is difficult for most balloon pins to lose contact with an object placed in a specific position or orientation, as shown in Fig. 6. Although the object in this simulation is limited to a rectangle, avoiding situations such as the one shown in Fig. 6 is important for the design of the proposed gripper because many real objects, particularly artifacts, have straight contours.

Increasing the expansion range of the balloon using a softer rubber material could prevent most balloon pins from failing to make contact; however, soft rubber materials stretch significantly when grasping heavy objects. Therefore, the situation shown in Fig. 6 cannot be completely ignored because a harder rubber should be used to increase the payload. Regarding balloon design, future research should clarify the appropriate rubber materials, considering hardness, durability, and friction, and methods for designing membrane thickness to control the shape during expansion.

The simulation model in this study has not considered the dynamics of the contact area between the gripper and object, and thus cannot fully reflect the behavior of the actual machine. However, notably, the characteristics of the proposed gripper were clarified to some extent using such a simple model. Furthermore, this evaluation method can be used not only for the balloon pin array gripper, but also for pin array grippers with a mechanism that expands uniformly around each pin, for example, using an origami structure.

Experimental comparisons with parallel-jaw grippers and multi-fingered grippers would be highly valuable for assessing the robustness of the proposed gripper against object misalignment. While this study focused solely on hardware aspects, future evaluations should consider the entire integrated system, including standard grasp detection software. Such comparisons under standardized conditions, such as uniform object properties and environmental lighting, will clarify how much the shape adaptability and isotropy of the proposed gripper contribute to robust grasping.

VI. CONCLUSION

In this letter, we introduce a balloon pin-array gripper that combines shape adaptability to various objects, stable holding by multipoint contact, and grasping performance independent of the object's position and orientation. Among the various aspects of the proposed gripper, this study focused on the influence of the pin layout on the grasping performance. The characteristics of each layout were quantified by a simulation focusing on multipoint contact, demonstrating the superiority of the concentric layout owing to its isotropy. The results of the experiments using the prototype gripper exhibited a trend consistent with the simulation results, and the validity of the simulation model was demonstrated. The proposed model can also be applied to characterize pin-array grippers with inflation mechanisms that are not limited to balloons.

Future studies will focus on fabricating grippers with the concentric layout, which demonstrated superiority in our simulations, to evaluate the robustness of the grasping performance. Additionally, mechanical improvements, such as enabling pins to detect contact and slide actively to minimize the forces exerted

on objects, will be pursued. Furthermore, we will investigate ways to increase the holding force by introducing high-friction materials such as gecko-like skin or by changing the stiffness of the balloon using smart fluids.

REFERENCES

- [1] F. Ilievski, A. D. Mazzeo, R. F. Shepherd, X. Chen, and G. M. Whitesides, "Soft robotics for chemists," *Angewandte Chemie Int. Ed.*, vol. 50, no. 8, pp. 1890–1895, Feb. 2011.
- [2] R. Deimel and O. Brock, "A novel type of compliant and underactuated robotic hand for dexterous grasping," *Int. J. Robot. Res.*, vol. 35, no. 1–3, pp. 161–185, Jan. 2016.
- [3] K. C. Galloway et al., "Soft robotic grippers for biological sampling on deep reefs," *Soft Robot.*, vol. 3, no. 1, pp. 23–33, Mar. 2016.
- [4] J. Zhou, S. Chen, and Z. Wang, "A soft-robotic gripper with enhanced object adaptation and grasping reliability," *IEEE Robot. Automat. Lett.*, vol. 2, no. 4, pp. 2287–2293, Oct. 2017.
- [5] S. Terryn, J. Brancart, E. Roels, G. Van Assche, and B. Vanderborght, "Room temperature self-healing in soft pneumatic robotics: Autonomous self-healing in a Diels-Alder polymer network," *IEEE Robot. Automat. Mag.*, vol. 27, no. 4, pp. 44–55, Dec. 2020.
- [6] W. Crooks, G. Vukasin, M. O'Sullivan, W. Messner, and C. Rogers, "Fin ray effect inspired soft robotic gripper: From the robosoft grand challenge toward optimization," *Front. Robot. AI*, vol. 3, Nov. 2016, Art. no. 70.
- [7] E. W. Schaler, D. Ruffatto, P. Glick, V. White, and A. Parness, "An electrostatic gripper for flexible objects," in *Proc. IEEE/RSJ Int. Conf. Intell. Robots Syst.*, 2017, pp. 1172–1179.
- [8] T. N. Do, H. Phan, T. Q. Nguyen, and Y. Visell, "Miniature soft electromagnetic actuators for robotic applications," Adv. Funct. Mater., vol. 28, no. 18, May 2018, Art. no. 1800244.
- [9] A. Pettersson, S. Davis, J. O. Gray, T. J. Dodd, and T. Ohlsson, "Design of a magnetorheological robot gripper for handling of delicate food products with varying shapes," *J. Food Eng.*, vol. 98, no. 3, pp. 332–338, Jun. 2010.
- [10] E. W. Hawkes, H. Jiang, D. L. Christensen, A. K. Han, and M. R. Cutkosky, "Grasping without squeezing: Design and modeling of shear-activated grippers," *IEEE Trans. Robot.*, vol. 34, no. 2, pp. 303–316, Apr. 2018.
- [11] G. Bancon and B. Huber, "Depression and grippers with their possible applications," in *Proc. 12th Int. Soc. Intell. Res.*, 1982, pp. 321–329.
- [12] J. R. Amend, E. Brown, N. Rodenberg, H. M. Jaeger, and H. Lipson, "A positive pressure universal gripper based on the jamming of granular material," *IEEE Trans. Robot.*, vol. 28, no. 2, pp. 341–350, Apr. 2012.
- [13] M. Fujita et al., "Jamming layered membrane gripper mechanism for grasping differently shaped-objects without excessive pushing force for search and rescue missions," Adv. Robot., vol. 32, no. 11, pp. 590–604, Jun. 2018.
- [14] Y. T. Choi, C. M. Hartzell, T. Leps, and N. M. Wereley, "Gripping characteristics of an electromagnetically activated magnetorheological fluid-based gripper," *Amer. Inst. Phys. Adv.*, vol. 8, no. 5, May 2018, Art. no. 056701.
- [15] K. Tadakuma et al., "The morphing omnidirectional gripper 'Morphing Omni-Gripper' with low melting point alloy," in *Proc. 26th Annu. Conf. Robot. Soc. Jpn.*, 2008, Art. no. 1E1-101.
- [16] S. Li et al., "A vacuum-driven origami 'magic-ball' soft gripper," in Proc. IEEE Int. Conf. Robot. Automat., 2019, pp. 7401–7408.
- [17] Y. Hao et al., "A multimodal, enveloping soft gripper: Shape conformation, bioinspired adhesion, and expansion-driven suction," *IEEE Trans. Robot.*, vol. 37, no. 2, pp. 350–362, Apr. 2021.
- [18] D. Wang, X. Wu, J. Zhang, and Y. Du, "A pneumatic novel combined soft robotic gripper with high load capacity and large grasping range," *Actuators*, vol. 11, no. 1, Dec. 2021, Art. no. 3.
- [19] P. B. Scott, "The 'Omnigripper': A form of robot universal gripper," *Robotica*, vol. 3, no. 3, pp. 153–158, Sep. 1985.
- [20] H. Fu and W. Zhang, "The development of a soft robot hand with pin-array structure," Appl. Sci., vol. 9, no. 5, Mar. 2019, Art. no. 1011.
- [21] A. Mo, H. Fu, C. Luo, and W. Zhang, "Concentric rotation pin array gripper for universal grasp," in *Proc. IEEE 3rd Int. Conf. Adv. Robot. Mechatron.*, 2018, pp. 112–117.
- [22] A. Mo and W. Zhang, "A novel universal gripper based on meshed pin array," *Int. J. Adv. Robot. Syst.*, vol. 16, no. 2, Mar. 2019, Art. no. 1729881419834781.
- [23] Y. Kemmotsu, K. Tadakuma, K. Abe, M. Watanabe, M. Konyo, and S. Tadokoro, "Balloon pin array gripper: Mechanism for deformable grasping with two-step shape adaptation," in *Proc. IEEE Int. Conf. Soft Robot.*, 2023, pp. 1–8.